Numerical Simulation of Flow and Heat Transfer of a Ferrofluid in a Partially Filled Porous Channel in a Gradient Magnetic Field

Amir Mokhtare[1], Amin Jafari[1], and Edward P. Furlani[1,2]

[1]Dept. of Chemical and Biological Engineering, [2]Dept. of Electrical Engineering,

University at Buffalo, The State University of New York, Buffalo NY

Email: efurlani@buffalo.edu

1 ABSTRACT

Unique interactions of ferrofluids with magnetic fields (MFs) can be exploited to achieve enhanced heat transfer for myriad fluidic based applications. In this study, we use numerical simulations to investigate the flow and heat transfer of a Fe_3O_4 ferrofluid in a vertical partially porous channel in the presence of a nonuniform (gradient) magnetic field provided by a permanent magnet. The flow is considered laminar and the Forchheimer–Brinkman extended Darcy model is used to predict flow through the porous region. The ferrofluid is heated as it flows upward in the vertical channel, mainly as it passes through the porous portion of the channel. The analysis shows that heat transfer enhancement for this system is predominantly due to three effects: the magnetic particles increase the effective thermal properties of the fluid, the porous medium provides a larger surface area that promotes heat transfer within the fluid and a nonuniform Kelvin body force within the ferrofluid produces vortices that disrupt the thermal boundary layer and stir the fluid. It is found that the fully-developed Nusselt number, which is a metric for heat transfer, can be practically doubled at the outlet. Furthermore, the modeling approach can be used for the rational design of novel heat exchanges.

Keywords: ferrofluid, magnetophoresis, ferrofluid transport in porous media, heat transfer enhancement, heat exchanger.

2 INTRODUCTION

Ferrofluids can be remotely manipulated using an applied magnetic field. This important feature is exploited in numerous applications in fields that include magnetic fluid hyperthermia, environmental engineering, drug delivery, nuclear fusion, chemical engineering, transformer cooling and more recently MEMS (micro-electro-mechanical systems), among many other [1, 2]. Another application of ferrofluids, which is the subject of this paper, is enhanced heat transfer. Finlayson [3] is among the pioneers in the field of thermomagnetic convection and has provided critical stability parameters beyond which this form of convection occurs. On the other hand, heat transfer enhancement using channels partially or totally filled with a porous medium has received extensive attention. The first such study was conducted by Beavers [4]. Hajipour implemented a comprehensive analysis on the mixed convection of a regular fluid and a nanofluid in channel containing porous media and viscous fluid regions. Porous metal foam heat exchangers are a preferred candidate for heat transfer applications. Specifically, metal foams hold great potential for optimum and compact heat exchangers because of their high effective surface area, fluid mixing qualities, and high thermal conductivity [5].

In this work, we use computational simulations to link the characteristics of the system, i.e. ferrofluid, partially porous medium and magnetic field, to enhance heat transfer. The porous medium is taken to be aluminum metal foam and the ferrofluid is a water-based solution with a 3% volume fraction of Fe_3O_4 nanoparticles. The magnetization of the ferrofluid is predicted using the nonlinear Langevin function. This multifaceted problem involves forced, free, and thermomagnetic convection together under a local thermal equilibrium (LTE) condition or equality of fluid and solid matrix temperatures. The Darcy–

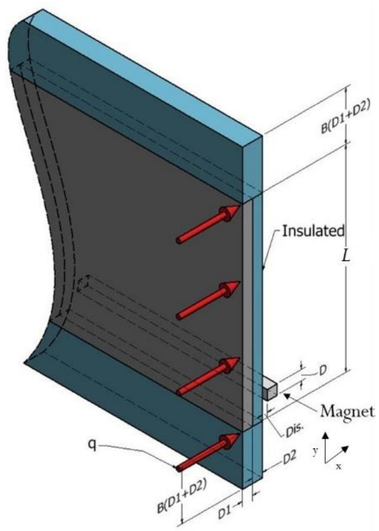

Figure 1. Schematic diagram of the partially filled porous channel (single permanent magnet).

Brinkman–Forchheimer model is used to predict flow in the porous medium. The magnetic field is generated by a permanent magnet and approximated as being two-dimensional. The significance of heat transfer analysis can be gauged by the value of the Nusselt number (Nu). Thus, the variation of Nu with respect to key system parameters is presented [6].

3 COMPUTATIONAL MODELS

A schematic diagram of the system and computational domain is shown in Error! Reference source not found.. The vertical channel of height L consists of a porous region of width D1 and free flow region of width D2. It is assumed that the interface of the porous and free region is located in the middle of the channel. The left wall is kept at a constant heat flux q and the right wall is thermally insulated. The ferrofluid flows upward, opposite to gravity, at the entrance region of the channel with a uniform velocity U_{in} and temperature T_{in}. The magnetic field is generated by a permanent magnet, which is adjacent to the free flow region as shown.

For nanoparticles less than 20 nm in diameter, the slip velocity between the particles and fluid is negligible and they are in thermal equilibrium. Therefore, the magnetic fluid can be considered as a single-phase system with average properties of its constituted phases [7]. The governing conservation equations for this problem can be written as follows: (subscripts p, f, and eq show porous, free, and equivalent properties of regions respectively and bold variables represent vector quantities) [8]:

- Continuity equation

$$\mathbf{\nabla}.\boldsymbol{v}_i = 0 \qquad i = p, f \tag{1}$$

- Momentum equation
  1. Porous region (D1 < x < 0):

$$\frac{\rho_f}{\varepsilon}\left(\frac{\partial \boldsymbol{v}_p}{\partial t} + \left(\boldsymbol{v}_p \cdot \mathbf{\nabla}\right)\frac{\boldsymbol{v}_p}{\varepsilon}\right) = -\nabla P + \frac{\mu}{\varepsilon}\mathbf{\nabla}^2\boldsymbol{v}_p + \rho\boldsymbol{g}\beta(T - T_0) + \mu_0(\boldsymbol{M}\cdot\mathbf{\nabla})\boldsymbol{H} - \frac{\mu}{K}\boldsymbol{v}_p - \frac{C_F\rho_f}{\sqrt{K}}\left|\boldsymbol{v}_p\right|\boldsymbol{v}_p \tag{2}$$

  2. Free flow region (0 < x < D2):

$$\rho_f\left(\frac{\partial \boldsymbol{v}_f}{\partial t} + \left(\boldsymbol{v}_f \cdot \mathbf{\nabla}\right)\boldsymbol{v}_f\right) = -\mathbf{\nabla}P + \mu\mathbf{\nabla}^2\boldsymbol{v}_f + \rho_f\boldsymbol{g}\beta(T - T_0) + \mu_0(\boldsymbol{M}\cdot\mathbf{\nabla})\boldsymbol{H} \tag{3}$$

- Energy equation
  1. Porous region (D1 < x < 0):

$$(\rho C_P)_{eq}\frac{\partial T}{\partial t} + \rho_f C_{P,f}\left(\boldsymbol{v}_p \cdot \mathbf{\nabla}\right)T = k_{eq}\mathbf{\nabla}^2 T - \mu_0 T\frac{\partial \boldsymbol{M}}{\partial T}\cdot\left(\left(\boldsymbol{v}_p\cdot\mathbf{\nabla}\right)\boldsymbol{H}\right) + \Phi_{v,p} \tag{4}$$

with

$$(\rho C_P)_{eq} = (1-\varepsilon)\rho_p C_{P,p} + \varepsilon\rho_f C_{P,f} \tag{5}$$

$$k_{eq} = (1-\varepsilon)k_p + k_f \tag{6}$$

$$\Phi_{v,p} = \frac{\mu}{K}\boldsymbol{v}_p\cdot\boldsymbol{v}_p + \frac{C_F\rho_f}{\sqrt{K}}\left|\boldsymbol{v}_p\right|\boldsymbol{v}_p\cdot\boldsymbol{v}_p \tag{7}$$

  2. Free flow region ($0 < \mathrm{x} < \mathrm{D}_2$):

$$\rho_f C_{P,f}\left(\frac{\partial T}{\partial t} + \left(\boldsymbol{v}_f\cdot\mathbf{\nabla}\right)T\right) = k_f\mathbf{\nabla}^2 T - \mu_0 T\frac{\partial \boldsymbol{M}}{\partial T}\cdot\left(\left(\boldsymbol{v}_f\cdot\mathbf{\nabla}\right)\boldsymbol{H}\right) + \mu\Phi_{v,f} \tag{8}$$

with

$$\Phi_{v,f} = \left(\mathbf{\nabla}\boldsymbol{v}_f + \left(\mathbf{\nabla}\boldsymbol{v}_f\right)^{tr}\right):\mathbf{\nabla}\boldsymbol{v}_f \tag{9}$$

- Magnetization equation

$$M = M_s\phi\left(coth(\xi) - \frac{1}{\xi}\right) \qquad \xi = \frac{\mu_0 V_{np} M_s H}{k_B T} \tag{10}$$

- Maxwell's magnetostatic equations

$$\mathbf{\nabla}\cdot\boldsymbol{B} = 0 \qquad \mathbf{\nabla}\times\boldsymbol{H} = 0 \qquad \boldsymbol{B} = \mu_0(\boldsymbol{H} + \boldsymbol{M}) \tag{11}$$

In the absence of the magnetic field and for low Reynolds numbers, the flow between the parallel plates, with $L/D = 4$ assures a fully developed laminar flow field. By adding a porous medium partially into the conduit the entrance length can be reduced by 50% or more [9]. For the sake of a consistent analysis, fully developed boundary conditions are assumed in both the absence and presence of the magnetic field. In this study, the height of channel is taken to be 20 times greater than the width of channel. The hydrodynamic and thermal boundary conditions based on these assumptions are shown in Figure 1

The local Nu value was calculated as follows

$$Nu = {q \times (D1 + D2)} \Big/ {keq(T_{w,avg} - T_{avg})} \qquad (12)$$

Where T_{avg} is the local mixing cup fluid temperature of the fluid at different heights of the channel. A parametric study is needed to evaluate the influence of a diverse range of parameters on design variables and the implementation of various fluid flow scenarios [10].

4 RESULTS & DISCUSSION

Ferrofluids under the influence of a magnetic field hold great potential for enhanced heat transfer technologies. Specifically, the synergistic effect of mixed convections and magnetization can be exploited to produce local mixing and vortexes in the fluid and enhance the heating or cooling phenomenon.

A schematic diagram of the streamlines of the magnetic field $\boldsymbol{H},$ i.e., are shown in Figure 2. Note that the field has a spatial gradient, which gives rise to body forces within the ferrofluid in both the x and y directions and associated velocity components that depend on the gradient of the MF as well as on the inlet velocity and temperature. Figure 3 shows the effects of different inlet velocities on the velocity profile inside the channel in the presence of the single permanent magnet with a residual magnetization of $M = 3 \times 10^5\ A/m$. As can be seen, the velocity profiles shift notably towards the MF source and vortices are created that are more significant when the inlet velocity is at its lowest level. The fluid rotation and

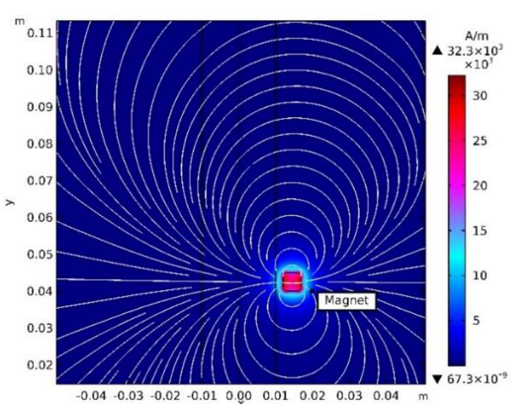

Figure 2. Magnetic field distribution of single permanent magnet ($M = 3 \times 10^5\ A/m$)

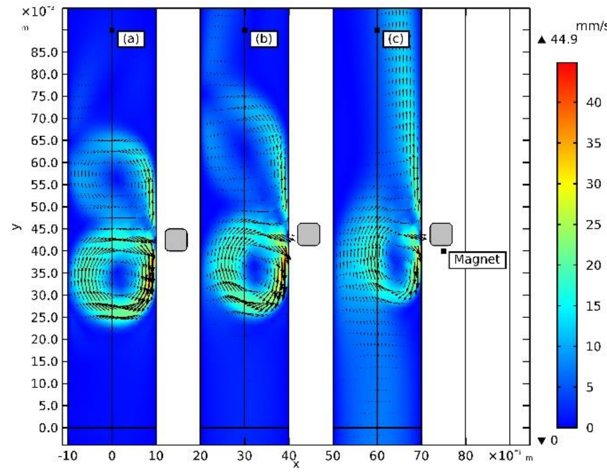

Figure 3. Velocity profile as a function inlet velocity in the presence of a single permanent magnet. a) $U_{in} = 0.05$ cm/s, b) $U_{in} = 0.15$ cm/s, c) $U_{in} = 0.5$ cm/s.

mixing efficiency are more pronounced for lower inlet velocities as well, which results in a greater temperature difference between the bulk average temperature and average wall temperature. According to the *Nu* number equation (12), this increased temperature difference results in an increase in the *Nu* values and therefore enhanced heat transfer.

The magnetization of the ferrofluid is proportional to reciprocal of the temperature. Hence, Kelvin body forces experienced by the colder parts of the fluid are larger than those experienced by the warmer regions of the fluid. This inequality in these Kelvin body forces leads to enhanced movement of the cold fluid toward the magnetic source and intensifies the local mixing of

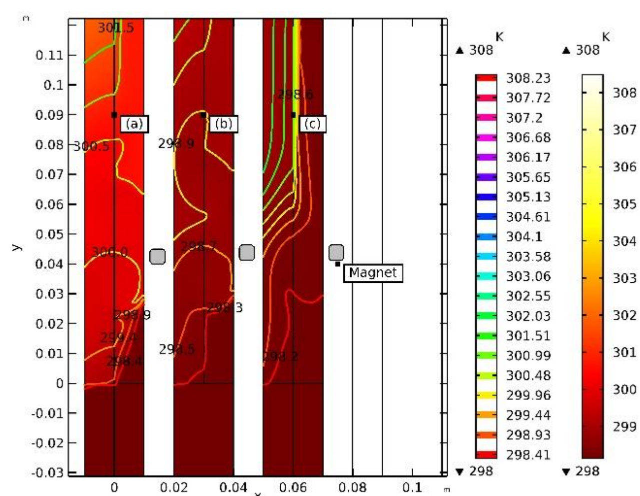

Figure 4. Effects of MF of the single permanent magnet on the temperature distribution in the channel as a function of the inlet velocity of fluid a) $U_{in} = 0.05$ cm/s, b) $U_{in} = 0.15$ cm/s, c) $U_{in} = 0.5$ cm/s.

the fluid and heat transfer near the magnetic source.

In the absence of the magnetic field and different inlet velocities, heat transfer rates (fully developed Nusselt numbers) are slightly greater than when water (solvent with no nanoparticles) was used. This increase is due to enhanced thermal properties of the fluid-nanoparticle mixtures. In the presence of the magnetic field, and with magnetic nanoparticles in the fluid, the local *Nu* values in the channel entrance zone increases. Significant improvements in the local *Nu* values are observed, which result is more efficient heat transfer rates.

Figure 4 shows how the rotational velocity profiles within the channel affect the temperature, i.e. by altering the thermal boundary layer that forms near the wall thereby facilitating heat transfer. The decrease in the thermal boundary layer resistance also enhances the heat transfer rates in the presence of the MF gradients

By increasing the magnetization of the magnet, a significant enhancement in the local *Nu* value along the height of the channel is achieved. Increasing the magnetization results in a redistribution of the fluid temperature profile and an increase in the local *Nu* values as shown in Figure 5.

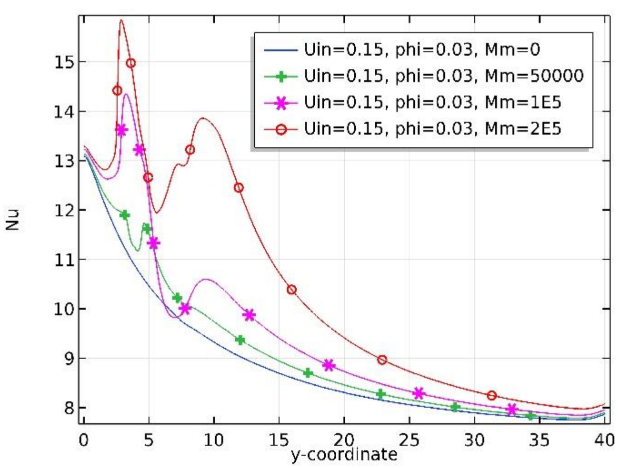

Figure 5. Nusselt number value vs. channel height as a function of the magnetization for the single permanent magnet

Our results also show that magnetic field has more of an effect on the pressure drop than on the total heat transfer. Hence, for applications where the heat transfer rate is more important than the pressure drop, an enhancement of heat transfer enhancement can be achieved with an acceptable increase in pressure drop.

5 CONCLUSION

We have investigated mixed convection heat tranfer in a partially porous parallel plate channel containing a ferrofluid in the presence of a nonuniform MF created by a single permanent magnet. We used computational parametric analysis to study the hydrothermal behavoir of the ferrofluid. We have found that heat transfer enhancement for this system is due to mainly to three effects: the magnetic particles increase the effective thermal properties of the fluid, the porous medium provides a larger heat transfer surface area within the fluid, and the nonuniform Kelvin body force with in ferrofluid produces vortices that disrupt the thermal boundary layer and stir the fluid. These effects result in an increase in the local *Nu* values and enhances the heat tranfer rates. Thus, ferrofluids hold a great potential for enhanced heat tranfer systems, which can be engineered for more efficient heating and cooling rates.

6 REFERENCES

[1] K. Liu *et al.*, *Physical Chemistry Chemical Physics,* 2017.

[2] T. Strek *et al.*, *Physica status solidi (b),* vol. 244, no. 3, pp. 1027, 2007.

[3] B. Finlayson, *Journal of Fluid Mechanics,* vol. 40, no. 4, pp. 753, 1970.

[4] G. S. Beavers *et al.*, *Journal of fluid mechanics,* vol. 30, no. 1, pp. 197, 1967.

[5] M. Hajipour *et al.*, *Heat Transfer—Asian Research,* vol. 43, no. 7, pp. 607, 2014.

[6] F. Fadaei *et al.*, *Applied Thermal Engineering,* vol. 116, pp. 329, 2017.

[7] R. Ganguly *et al.*, *Physics of Fluids,* vol. 16, no. 7, pp. 2228, 2004.

[8] E. Purlani, *Analysis and Applications (New York: Academic),* 2001.

[9] B. A. Finlayson, *Physics of Fluids,* vol. 25, no. 7, p. 073101, 2013.

[10] F. Fadaei *et al.*, *J Magn Magn Mater,* vol. 429, pp. 314, 2017.